ANALYSIS OF OSTEOBLAST-LIKE MG63 CELLS' RESPONSE TO A ROUGH IMPLANT SURFACE BY MEANS OF DNA MICROARRAY

Francesco Carinci, MD
Furio Pezzetti, PhD
Stefano Volinia, PhD
Francesca Francioso, PhD
Diego Arcelli, PhD
Jlenia Marchesini, PhD
Luca Scapoli, PhD
Adriano Piattelli, MD

KEY WORDS

DNA microarray
Expression profiling
Implant surface
Titanium

Francesco Carinci, MD, *is an associate professor of maxillofacial surgery at the University of Ferrara, Italy.*

Furio Pezzetti, PhD, *is an associate professor of histology, Institute of Histology, University of Bologna, and Centre of Molecular Genetics, CARISBO Foundation, Italy.*

Stefano Volinia, PhD, *is an assistant professor of histology;* ***Francesca Francioso, PhD,*** *is a student;* ***Diego Arcelli, PhD,*** *is a postdoctoral fellow; and* ***Jlenia Marchesini, PhD,*** *is a student in the Department of Morphology and Embryology, University of Ferrara, Italy.*

Luca Scapoli, PhD, *is a postdoctoral fellow at the Institute of Histology, University of Ferrara, Italy.*

Adriano Piattelli, MD, *is a full professor and dean of the Dental School, Via F. Sciucchi 63, 66100 Chieti, Italy (e-mail: apiattelli@unich.it). Address correspondence to Dr Piattelli.*

Several features of the implant surface, such as composition, topography, roughness, and energy, play a relevant role in implant integration with bone. Little is known about the structural and chemical surface properties that may influence biological responses. Expression profiling by DNA microarray is a molecular technology that allows the analysis of gene expression in a cell system. By using DNA microarrays containing 19 200 genes, we identified several genes whose expression was significantly down-regulated in osteoblast-like cell line MG63 on a new implant surface (titanium pull spray superficial [TPSS] surface, Oralplant, Cordenons, PN, Italy). The differentially expressed genes cover a broad range of functional activities: (1) signaling transduction, (2) translation, (3) cell cycle regulation, (4) structural and metabolic functions, and (5) apoptosis. It was also possible to detect some genes whose functions are unknown. The data reported can be relevant to better understand the role of the type of surface on the molecular mechanism of implant osseointegration and as a model for comparing other materials.

INTRODUCTION

Several features of the implant surface such as composition, topography, roughness, and energy play a relevant role in implant integration with bone.[1–21] Little is known about the structural and chemical surface properties that may influence biological responses.[1] Surface roughness has been demonstrated to have positive effects on adsorption of molecules, local factor production, and proliferation and differentiation of cells.[13,14,22] The optimal value for the implant surface roughness is still to be determined, but it has been suggested that irregularities in the 1.5 μm range probably result in a higher bone implant contact percentage.[4] Titanium has been widely used in the biomedical field, but the factors and mechanisms underlying the biological response to titanium are not yet well understood,[1] and it is necessary to look for correlations between surface characteristics and response of biologic tissues at different levels of resolution and sophistication.[1]

DNA microarray is a molecular technology that enables the analysis of gene expression in parallel with a very

large number of genes, spanning a significant fraction of the human genome. It is a qualitative analysis (eg, it can differentiate each single gene) as well as quantitative, since it has the sensitivity to detect a change of expression level in the investigated cells when compared with normal samples. Technically, reference RNA (eg, cells cultured on machined titanium) and investigated RNA (eg, cells cultured on a specific titanium surface) are labeled after reverse transcription with different fluorescent dyes (Cy3 for the reference cells and Cy5 for the investigated cells) and hybridized to a cDNA microarray containing robotically printed cDNA fragments. The slides are then scanned with a laser scanning system, and 2 false color images are generated for each hybridization with RNA from the investigated and reference cells. Genes up-regulated in the investigated cells are conventionally designated red, whereas those with decreased expression appear green, since more are expressed in the normal sample. Genes with similar levels of expression in the 2 samples appear yellow. The overall result is the generation of a so-called genetic portrait.[23,24]

In the present study we defined the effects of a new implant surface on genes by using an osteoblast-like cell line (MG63) and microarray slides containing 19 200 different oligonucleotides.

MATERIALS AND METHODS

Cell culture

Osteoblast-like cells (MG63) were cultured in sterile Falcon wells (Becton Dickinson, NJ) containing Eagle's minimum essential medium (MEM) supplemented with 10% fetal calf serum (FCS; Sigma Chemical Co, St Louis, Mo) and antibiotics (Penicillin 100 U/mL and Streptomycin 100 μg/mL; Sigma). Cultures were maintained in a 5% CO_2 humidified atmosphere at 37°C.

MG63 cells were collected and seeded at a density of 1×10^5 cells/mL into 9 cm^2 (3 mL) wells by using 0.1% trypsin, 0.02% EDTA in Ca++, and Mg-free Eagle's buffer for cell release. One set of wells contained sterile metal disks of machined grade 3 titanium (diameter 3 cm, control implants), whereas another contained titanium implants with a new surface (titanium pull spray superficial [TPSS] surface; Oralplant, Cordenons, PN, Italy) covering the same area (35 cm^2). This new surface was produced through micromechanical removal of parts of the superficial oxide layer with the use of aluminum oxide 0.5 μm/micropoints. The Ra value was 0.30 for the machined surface and 2.74 for the TPSS surface. After 24 hours, the medium (3 mL of MEM with 10% FCS) was changed. Finally, after 24 hours the cultures reached subconfluence and the cells were processed for RNA extraction.

DNA microarrays screening and analysis

RNA was extracted from the cells by using RNAzol. Ten micrograms of total RNA were used for each sample. Complementary DNA was synthesized by using Superscript II (Life Technologies, Invitrogen, Milano, Italy) and aminoallyl dUTP (Sigma). Mono-reactive Cy3 and Cy5 esters (Amersham Pharmacia) were used for indirect cDNA labeling. RNA extracted from cells grown on machined titanium disks was labeled with Cy3 and used as control against the Cy5-labeled, treated (TPSS titanium surface) cDNA in the first experiment and then switched. Human 19.2 K DNA microarrays were used (Ontario Cancer Institute). For 19.2 K slides, 100 μL of the sample and control cDNAs in DIG Easy hybridization solution (Roche) were used in a sandwich hybridization of the 2 slides, which constituted the 19.2. K set at 37°C overnight. Washing was performed 3 times for 10 minutes with 1 × sodium dodecyl sulfate (SSC), 0.1% SSC at 42°C, and 3 times for 5 minutes with 0.1 × SSC at room temperature. Slides were dried by centrifugation for 2 minutes at 2000 rpm. The experiment was repeated twice and the dyes switched. A GenePix 4000a DNA microarrays scanner (Axon, Union City, Calif) was used to scan the slides, and data were extracted with GenePix Pro. After removing local background, genes with expression levels of less than 1000 were not included in the analysis, since ratios are not reliable at that detection level.[23,24]

RESULTS

DNA microarrays

After scanning the 2 slides containing the 19 200 human genes in duplicate, local background was calculated for each target location. A normalization factor was estimated from ratios of median. Normalization was performed by adding the $\log_2$ of the normalization factor to the $\log_2$ of the ratio of medians. The $\log_2$ ratios for all the targets on the array were then calibrated using the normalization factor, and $\log_2$ ratios outside the 99.7% confidence interval (the median ±3 times the SD = 0.52) were determined as significantly changed in the treated cells. Thus genes are significantly modulated in expression when the absolute value of their $\log_2$ expression level is higher than 1.56, or else there is a threefold difference in expression between treated cells and the reference. GenePix Pro software was used to report genes above the threshold and with less than 10% difference in 3 different statistical evaluations of the intensity ratio, thus effectively enabling an automated quality control check of the hybridized spots. Furthermore, all of the positively passed spots were finally visually inspected. Generally, no further exclusion was needed at this final step, since the previously applied automated selection filters were highly stringent.[23,24]

The significance analysis of microarray (SAM) program was then performed, and a SAM score was obtained (*t*-statistic value). The down-regulated genes differentially expressed in the machined and the TPSS implant sur-

TABLE 1

Clone ID	UG Cluster	Name	Symbol	Chromosome	Score
39884	Hs. 850	IMP (inosine monophosphate) dehydrogenase 1	IMPDH1	7q31.3-q32	−4.2706
206340	Hs. 154583	RNA binding motif protein 10	RBM10	Xp11.23	−3.40215
40306	Hs. 25882	Gemin 5	GEMIN5	5q34	−3.02111
245002	Hs. 24049	Golgi autoantigen, golgin subfamily a, 2	GOLGA2	9q34.13	−2.89537
133037	Hs. 79946	Cytochrome P450, subfamily XIX (aromatization of androgens)	CYP19	15q21.1	−2.83403
47197	Hs. 239176	Insulin-like growth factor 1 receptor	IGF1R	15q25-q26	−2.66806
149046	Hs. 28346	Glial cells missing homolog 1 (Drosophila)	GCM1	6p21-p12	−2.5961
229878	Hs. 282847	Pregnancy specific β-1-glycoprotein 1	PSG1	19q13.2	−2.56923
33980	Hs. 279609	Mitochondrial carrier homolog 2	MTCH2	11q12.1	−2.49114
40076	Hs. 7731	Uncharacterized bone marrow protein BM036	BM036	14q12	−2.45249
268260	Hs. 75511	Connective tissue growth factor	CTGF	6q23.1	−2.21133
37166	Hs. 82587	Phospholipase D1, phophatidylcholine-specific	PLD1	3q26	−2.2003
342113	Hs. 343696	Trigger transposable element derived 7	TIGD7	16p13.11	−2.15262
231010	Hs. 61271	Hypothetical protein FLJ21159	FLJ21159	4q31.3	−2.13078
488877	Hs. 50651	Janus kinase 1 (a protein tyrosine kinase)	JAK1	1p32.3-p31.3	−2.11654
245662	Hs. 1901	Kallikrein B, plasma (Fletcher factor) 1	KLKB1	4q34-q35	−2.08815
222237	Hs. 240112	KIAA0276 protein	KIAA0276	4p12	−2.07966
235958	Hs. 187958	Solute carrier family 6 (neurotransmitter transporter, creatine), member 8	SLC6A8	Xq28	−2.07024
206345	Hs. 112255	Nucleoporin 98kDa	NUP98	11p15.5	−2.02611
124941	Hs. 283771	Chromosome 21 open reading frame 66	C21orf66	21q21.3	−2.01147
113357	Hs. 105749	KIAA0553 protein	KIAA0553	17q21.31	−2.00158
42170	Hs. 246857	Mitogen-activated protein kinase 9	MAPK9	5q35	−2.00068
382694	Hs. 8024	IK cytokine, down-regulator of HLA II	IK	5q31.3	−1.98835
279488	Hs. 89666	A kinase (PRKA) anchor protein 6	AKAP6	14q12	−1.98033
489344	Hs. 10760	Asporin (LRR class 1)	ASPN	9q22	−1.95879
240655	Hs. 308026	Major histocompatibility complex, class II, DR β 3	HLA-DRB3	6p21.3	−1.93531
246497	Hs. 37636	Hypothetical protein FLJ25162	FLJ2516	10q22.2	−1.93094
233177	Hs. 154145	Metallo phosphoesterase	MPPE1	18p11.21-p11.	−1.92261
665047	Hs. 57301	MutL Homolog 1, colon cancer, nonpolyposis type 2 (*E coli*)	MLH1	3p21.3	−1.92129
488246	Hs. 172870	KIAA1913 protein	KIAA1913	6q23.1	−1.90943
25396	Hs. 20935	Hypothetical protein DKFZp761D221	DKFZp761D221	1p31.2	−1.88086
430255	Hs. 60389	ESTs			−3.24727
239524	Hs. 20799	ESTs			−2.63869
230507	Hs. 408754	ESTs			−2.44052
244896	Hs. 269084	ESTs			−2.36071
277063	Hs. 82415	ESTs			−2.34861
231461	Hs. 196008	ESTs			−2.161
241587	Hs. 302965	ESTs			−2.03048
161788	Hs. 381543	Ests, Moderately similar to PRO0478 protein (*Homo sapiens, H sapiens*)			−2.02217
234697	Hs. 407926	ESTs			−1.94007
239534	Hs. 37560	ESTs			−1.93929
113275	Hs. 409343	ESTs			−1.89644
200272	Hs. 347143	ESTs, Weakly similar to hypothetical protein FLJ20294 (*Homo sapiens, H sapiens*)			−1.88057
212331	Hs. 205980	ESTs			−1.82693

face are reported in Tables 1 and 2 and in the Figure.

DISCUSSION

Hybridization of mRNA-derived probes to cDNA microarrays allows us to perform systemic analysis of expression profiles for thousands of genes simultaneously and to provide primary information on transcriptional changes related to an implant surface (TPSS surface; Oralplant). We identified several genes whose expression was definitely down-regulated (Table 1).

Transduction

The insulin-like growth factor 1 receptor (IGF1R) binds insulin-like growth factor with a high affinity. It has tyrosine kinase activity and plays a critical role in transformation events. Cleavage of the precursor generates α and β subunits. It is highly overexpressed in most malignant tissues, where it functions as an antiapoptotic agent by enhancing cell survival. It is down-regulated by this implant surface.[25] Also, the connective tissue growth factor (CTGF) is down-regulated by the TPSS surface. CTGF binds IGF and may have a role in regulating normal and neoplastic cell growth.[26]

Janus kinase 1 (JAK1), is a member of a new class of protein-tyrosine kinases (PTK), is characterized by the presence of a second phosphotransferase-related domain immediately N-terminal to the PTK domain. The second phosphotransferase domain bears all the hallmarks of a protein kinase, although its structure differs significantly from that of the PTK and threonine/

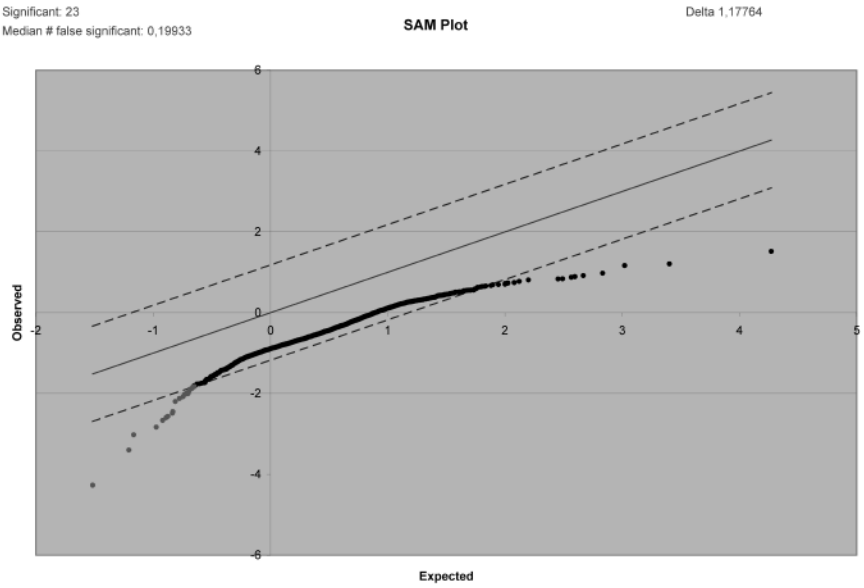

FIGURE. Result of 1 of the 2 slides containing 19.200 genes: 23 different genes are significantly down-regulated (in the lower left square). The *y*-axis displays the observed cases, whereas the *x*-axis depicts the expected. The graphic has a $\log_2$ scale. A normalization factor was estimated from ratios of median. Normalization was performed by adding the $\log_2$ of the normalization factor to the $\log_2$ of the ratio of medians. The $\log_2$ ratios for all the targets on the array were then calibrated using the normalization factor, and $\log_2$ ratios outside the 99.7% confidence interval (the median ±3 times the SD = 0.52) were determined as significantly changed.

serine kinase family members. JAK1 is a large, widely expressed membrane-associated phosphoprotein. JAK1 is involved in the interferon-α, -β, and -γ signal transduction pathways. The reciprocal interdependence between JAK1 and TYK2 activities in the interferon-α pathway, and between JAK1 and JAK2 in the interferon-γ pathway, may reflect a requirement for these kinases in the correct assembly of interferon receptor complexes. These kinases couple cytokine ligand binding to tyrosine phosphorylation of various known signaling proteins and of a unique family of transcription factors, which are termed the signal transducers and activators of transcription, or STATs.[27]

Translation

Signal-mediated nuclear import and export proceeds through the nuclear pore complex, which is comprised of approximately 50 unique proteins collectively known as nucleoporins. The 98 kD nucleoporin (NUP98) functions as 1 of several docking site nucleoporins of transport substrates and is down-regulated by the new implant surface.[28]

Cell cycle

Inosine-5′-monophosphate dehydrogenase (IMPDH1) catalyzes the formation of xanthine monophosphate (XMP) from IMP. In the purine de novo synthetic pathway, IMP dehydrogenase is positioned at the branch point in the synthesis of adenine and guanine nucleotides and is thus the rate-limiting enzyme in the de novo synthesis of guanine nucleotides. Inhibition of cellular IMP dehydrogenase activity results in an abrupt cessation of DNA synthesis and a cell cycle block at the G1-S interface.[29]

Enzyme and cytoskeleton

Phosphatidylcholine (PC)-specific phospholipases D (PLDs) catalyze the hydrolysis of PC to produce phosphatidic acid and choline. A range of agonists acting through G protein-coupled receptors and receptor tyrosine kinases stimulate this hydrolysis. PC-specific PLD activity has been implicated in numerous cellular pathways, including signal transduction, membrane trafficking, and the regulation of mitosis. Hammond et al[30] showed that recombinant PLD1 activity is located both in the cytoplasm and in association with the membrane; they suggested that PLD1 can exist as a stable soluble protein and that controlled interaction with substrate-containing phospholipid surfaces may be a physiologically important mode of regulation. The same authors found that ADP-ribosylation factor-1 (ARF1) activates PLD1, suggesting that PLD1 is involved in intravesicular membrane trafficking.

The A-kinase anchor proteins (AKAPs) are a group of structurally diverse proteins, which have the common function of binding to the regulatory subunit of protein kinase A (PKA) and confining the holoenzyme to discrete locations within the cell. AKAP6 encodes a member of the AKAP family. The encoded protein is highly expressed in various brain regions and cardiac and skeletal muscle. It is specifically localized to the sarcoplasmic reticulum and nuclear membrane and is involved in anchoring PKA to the nuclear membrane or sarcoplasmic reticulum.[31]

Apoptosis

MAPK9 is a member of the mitogen-activated protein (MAP) kinase family. MAP kinases act as an integration point for multiple biochemical signals and are involved in a wide variety of cellular processes such as proliferation, differentiation, transcription regulation, and development. This kinase targets specific transcription factors, and thus mediates immediate-early gene expression in response to various cell stimuli. It is most closely related to MAPK8, both of which are involved in ultraviolet (UV) radiation-induced apoptosis, which is thought to be related to the cytochrome c-mediated cell death pathway. This gene and MAPK8 are also known as c-Jun N-terminal kinases. This kinase blocks the ubiquitin-

ation of tumor suppressor p53, and thus it increases the stability of p53 in nonstressed cells.[32]

The genes discussed are only a limited number among those differentially expressed and reported in Table 1. We briefly analyzed some of those with a better-known function. There are also a number of expressed sequence tags (EST) whose function is unknown (Table 2). However, the recognition of altered expression of specific EST can help give it a role.

In conclusion, we have shown that the new implant surface is able to modulate the expression of some genes that cover a broad range of functional activities: (1) signaling transduction, (2) translation, (3) cell cycle regulation, (4) enzyme and cytoskeleton development, and (5) apoptosis.

Recent studies on animal models have demonstrated that titanium surfaces are of paramount importance in influencing the timing of bone healing, and rougher surfaces have been demonstrated to present a higher quantity of bone-implant contact percentage and higher removal torque values.[6,7,10,11,22] The surface roughness has been demonstrated to alter the responsiveness of different types of cells.[8,13,14] However, because the in vitro system differs from the in vivo system, more investigations are needed. Indeed, MG63 are osteoblast-like cells and not normal osteoblast, and a monolayer cell stratum differs significantly from bone tissue, where osteoblasts are resident in a bone matrix. Moreover, some differences between the genetic portrait reported and genes described by different authors may be related to the chosen time point of the experiment. We chose to perform the experiment after 24 hours of stimulation in order to get information on the early stages of stimulation. It is our belief, however, that more investigations with different osteoblast-like cell lines, primary cultures, and time points are needed in order to get a better comprehension of the molecular events related to the interaction between the surface and the osseointegration process. Finally, we believe that the reported data can be a model to compare different implant surfaces.

Acknowledgments

This work was supported by grants from Unife 60% (F.C.), Guya-Bioscience, and the CARISBO Foundation (F.P.).

References

1. Larsson C, Thomsen P, Aronsson BO, Rodahl M, Lausmaa J, Kasemo B, Ericsson LE. Bone response to surface-modified titanium implants: studies on the early tissue response to machined and electropolished implants with different oxide thicknesses. *Biomaterials.* 1996;17:605–610.

2. Puleo DA, Nanci A. Understanding and controlling the bone-implant interface. *Biomaterials.* 1999;20: 2311–2321.

3. Bowers KT, Keller J, Randolph BA, Wick DG, Michaels CM. Optimization of surface micromorphology for enhanced osteoblast responses in vitro. *Int J Oral Maxillofac Implants.* 1992;7: 302–310.

4. Han CH, Johansson CB, Wennenberg A, Albrektsson T. Quantitative and qualitative investigations of surface enlarged titanium and titanium alloys implants. *Clin Oral Implant Res.* 1998;9:1–10.

5. Cooper LF, Masuda T, Whitson W, Yliheikkila P, Felton DA. Formation of mineralizing osteoblast cultures on machined, titanium oxide grit-blasted, and plasma-sprayed titanium surfaces. *Int J Oral Maxillofac Implants.* 1999;14: 37–47.

6. Klokkevold P, Nishimura RD, Adachi M, Caputo A. Osseointegration enhanced by chemical etching of the titanium surface. A torque removal study in the rabbit. *Clin Oral Implant Res.* 1997;8:442–447.

7. Gotfredsen K, Wennerberg A, Johansson C, Skovgaard LT, Hjorting-Hansen E. Anchorage of TiO_2-blasted, HA-coated and machined implants: an experimental study with rabbits. *J Biomed Mater Res.* 1995;29:1223–1231.

8. Park JY, Davies JE. Red blood cell and platelet interactions with titanium implant surfaces. *Clin Oral Implant Res.* 2000;11:530–539.

9. Mustafa K, Wroblewski J, Hultenby K, Silva Loprez B, Arvidson K. Effects of titanium surfaces blasted with TiO_2 particles on the initial attachment of cells derived from mandibular bone. A scanning electron microscopic and histomorphometric analysis. *Clin Oral Implant Res.* 2000;11:116–128.

10. Wennerberg A, Albrektsson T, Lausmaa J. Torque and histomorphometric evaluation of c.p. titanium screws blasted with 25- and 75 m-sized particles of Al_2O_3. *J Biomed Mater Res.* 1996;30:251–260.

11. Wennerberg A, Albrektsson T, Johansson C, Andersson B. Experimental study of turned and grit-blasted screw-shaped implants with special emphasis on effects of blasting material and surface topography. *Biomaterials.* 1996;17:15–22.

12. Mustafa K, Lopez BS, Hultenby K, Wennenberg A, Arvidson K. Attachment and proliferation of human oral fibroblasts to titanium surfaces blasted with TiO_2 particles. A scanning electron microscopic and histomorphometric analysis. *Clin Oral Implant Res.* 1998; 9:195–207.

13. Schwartz Z, Martin JY, Dean DD, Simpson J, Cochran DL, Boyan BD. Effect of titanium surface roughness on chondrocyte proliferation, matrix production, and differentiation depends on the state of cell maturation. *J Biomed Mater Res.* 1996;30:145–155.

14. Martin JY, Schwartz Z, Hummert TW, et al. Effect of titanium surface roughness on proliferation, differentiation, and protein synthesis of human osteoblast-like cells (MG 63). *J Biomed Mater Res.* 1995;29:389–401.

15. Den Braber ET, De Ruijter JE, Smits HTJ, Ginsel LA, Von Recum AF, Jansen JA. Effect of parallel surface microgrooves and surface energy on cell growth. *J Biomed Mater Res.* 1995;29: 511–518.

16. Wennenberg A, Hallgren C, Jo-

hansson C, Danelli S. A histomorphometric evaluation of screw-shaped implants each prepared with two surface roughnesses. *Clin Oral Implant Res.* 1998;9:11–19.

17. Feighan JE, Goldberg VM, Davy D, Parr JA, Stevenson S. The influence of surface-blasting on the incorporation of titanium-alloy implants in a rabbit intramedullary model. *J Bone Joint Surg*. 1995;77-A:1380–1395.

18. Chehroudi B, McDonnel D, Brunette DM. The effects of micromachined surfaces on formation of bone-like tissue on subcutaneous implants as assessed by radiography and computer image processing. *J Biomed Mater Res.* 1997;34:279–290.

19. Piattelli A, Manzon L, Scarano A, Paolantonio M, Piattelli M. Histologic and morphologic analysis of the bone response to machined and sandblasted titanium implants: an experimental study in rabbit. *Int J Oral Maxillofac Implants.* 1998;13:805–810.

20. Piattelli M, Scarano A, Paolantonio M, Iezzi G, Petrone G, Piattelli A. Bone response to RBM sandblasted titanium implants: an experimental study in rabbit. *J Oral Implantol.* 2002; 28:2–8.

21. Wennenberg A, Albrektsson T, Andersson B. An animal study of c.p. titanium screws with different surface topographies. *J Mater Sci: Mater M.* 1995;6:302–309.

22. Gotfredsen K, Berglundh T, Lindhe J. Anchorage of titanium implants with different surface characteristics: an experimental study in rabbits. *Clin Implant Dent Relat Res.* 2000;2:120–129.

23. Francioso F, Carinci F, Tosi L, et al. Identification of differentially expressed genes in human salivary gland tumors by DNA microarrays. *Mol Cancer Ther.* 2002;1:533–538.

24. Carinci F, Francioso F, Rubini C, et al. Genetic portrait of malignant granular cell odontogenic tumour. *Oral Oncol.* 2003;39:69–77.

25. Werner H, Karnieli E, Rauscher FJ III, LeRoth D. Wild-type and mutant p53 differentially regulate transcription of the insulin-like growth factor I receptor gene. *Proc Nat Acad Sci.* 1996; 93:8318–8323.

26. Kim HS, Nagalla SR, Oh Y, Wilson E, Roberts CT Jr, Rosenfeld RG. Identification of a family of low-affinity insulin-like growth factor binding proteins (IGFBPs): characterization of connective tissue growth factor as a member of the IGFBP superfamily. *Proc Natl Acad Sci.* 1997;94:12981–12986.

27. Ihle JN. Cytokine receptor signaling. *Nature.* 1995;377:591–594.

28. Enninga J, Levy DE, Blobel G, Fontoura BMA. Role of nucleoporin induction in releasing an mRNA nuclear export block. *Science.* 2002;295:1523–1525.

29. Natsumeda Y, Ohno S, Kawasaki H, Konno Y, Weber G, Suzuki K. Two distinct cDNAs for human IMP dehydrogenase. *J Biol Chem.* 1990;265: 5292–5295.

30. Hammond SM, Altshuller YM, Sung TC, et al. Human ADP-ribosylation factor-activated phosphatidylcholine-specific phospholipase D defines a new and highly conserved gene family. *J Biol Chem.* 1995;270:29640–29643.

31. Kapiloff MS, Schillace RV, Westphal AM, Scott JD. mAKAP: an A-kinase anchoring protein targeted to the nuclear membrane of differentiated myocytes. *J Cell Sci.* 1999;112:2725–2736.

32. Tournier C, Hess P, Yang DD, et al. Requirement of JNK for stress-induced activation of the cytochrome c-mediated death pathway. *Science.* 2000; 288:870–874.